# FIELD-BASED CLASSIFICATION OF AGRICULTURAL CROPS USING MULTI-SCALE IMAGES

A. OZDARICI [a] , M. TURKER[b]

[a] Middle East Technical University (METU), Graduate School of Natural and Applied Sciences, Geodetic and Geographic Information Technologies, 06531-Ankara, TURKEY, email: ozdarici@metu.edu.tr

[b] Hacettepe University, Faculty of Engineering, Department of Geodesy and Photogrammetry, Beytepe, 06800 Ankara, TURKEY, email: mturker@hacettepe.edu.tr

**Commission VI, WG VI/4**

KEY WORDS: Field-Based Image Classification, High Resolution, Agricultural Crop Mapping, SPOT4, SPOT5, IKONOS, QuickBird, Turkey

**ABSTRACT:**

This paper presents field-based classifications performed using the multi-resolution images of SPOT4 XS, SPOT5 XS, IKONOS XS, QuickBird XS, and QuickBird Pansharpaned (PS) covering an agricultural area located in Karacabey, Turkey. The objective was to assess the classification accuracies of different spatial resolution images in an agricultural land using the field-based classification techniques. To do that pre-field classification was performed using the common bands of the images. For each field, the statistical measures of the mean, median, and mode values were calculated. Then, a Maximum Likelihood Classification (MLC) was carried out using the derived bands. After computing the accuracies of the classifications, it was observed that similar results were obtained, for each image, when the mean values were used. Of the images used, the 0.61m resolution QuickBird PS image provided the highest overall accuracy of 85.2% using the median bands classification. On the other hand, the lowest overall accuracy was found to be 42.9%, when the SPOT4 XS image was classified using the median bands.

## 1. INTRODUCTION

Remote Sensing (RS) is an effective technology to collect information about geographic objects. With the recent advances in RS technology, the high spatial resolution images, such as acquired by the SPOT5, IKONOS, and QuickBird satellites have become widely available. As increasing number of higher resolution satellite images become available, the selection of the appropriate spatial resolution becomes more complex. This is because appropriate spatial resolution is a function of the measure of environment, the kind of information desired and the techniques used to extract information (Chen *et al*., 2004). Of the many application areas, the agricultural activities require a quantitative processing of remote sensing data with high accuracy and reliability. The agricultural activities, such as crop mapping, environmental modelling, yield estimation and updating provide significant information for marketing and trading decisions.

Automated image classification is a commonly used technique to extract information from earth surface features. Image classification can be performed using two methods: (i) pixel-based, and (ii) field-based. In the conventional pixel-based classification, the pixels are categorized separately into one of the pre-determined classes according to their spectral characteristics. However, in the case of agricultural applications, pixel-based classification techniques may cause problems due, for example, to the variations in soil moisture conditions, nutrient limitations or pests and diseases. On the other hand, spectral confusions may occur due to the mixed pixels located on the boundary of two or more land cover types (De Wit and Clevers, 2004). Therefore, when the classification is performed on per-pixel basis, these factors may cause to assign a combination of the reflectance from two or more land cover types. And, this causes misclassification (Smith and Fuller, 2001).

The basic idea behind a field-based classification is that the image is divided into homogenous objects using the knowledge of existing agricultural field boundaries. With regard to crop classification, this means that the location and the extent of each field are known apriori. During classification, each pixel is assigned to a final class of the entire object according to their statistical properties, instead of determining the class label for each pixel separately. Therefore, field-based methods eliminate the effect of the spectral variability within the fields and the mixed pixels falling on field boundaries (De Wit and Clevers, 2004). Thus, for detecting the crop types, field-based classification techniques produce more reliable results than the conventional pixel-based classification techniques by overcoming the problems of misclassification.

Field-based image classification can be carried out at two moments in the classification procedure: (i) pre-field classification, and (ii) post-field classification. In pre-field classification, the statistical measures such as, the mean, median and mode values are calculated per-field. The pixel values in each field are then replaced with the computed statistical value and the image is classified on pixel-based manner. In post-field classification, first, a pixel-based classification is carried out. Then, for each field, the frequency of the classified pixels is

computed and the majority class is assigned as the label of the field.

The objective of this study is to compare the classification accuracies of the multi-resolution images in an agricultural land using the pre-field classification technique. To perform the classification and evaluate the results, a study area located in the Karacabey Plain in northwest of Turkey was selected. The study was carried out using five satellite images that are SPOT4 XS (20m), SPOT5 XS (10m), IKONOS XS (4m), Quickbird XS (2,44m) and QuickBird Pansharpaned (0,61m). For these images, the common bands (Green, Red and Near-Infrared) were used to make the comparison of the results more reliably and accurately. First, the preprocessing operations were carried out. These include updating the vector field boundary data, data fusion, and geometric corrections. Upon completing the preprocessing operations, the pre-field classifications of the images were performed. To do that, first, the vector and raster data were integrated. Then, for each field, the mean, median, and mode values were calculated. Next, these values were replaced by the original pixel values and, for each image, the MLC was performed. To invoke the queries effectively for assessing the results, a database was utilized. Finally, the classified images were assessed using the reference data and their accuracies were compared.

## 2. STUDY AREA AND DATA DESCRIPTION

The study area is located in Marmara region near the town of Karacabey located in northwest of Turkey (Figure 1). The area lies between the latitudes 4 444 750.00 N to 4 453 500.00 N and longtitudes 610 750.00 E to 599 850.00 E. It covers an area of approximately 95 $km^2$. The area is representative of the agricultural structure and it is one of the most valuable agricultural regions of Turkey. There are multiple crop types with multiple growing seasons in the area. The main crops cultivated in the area include tomato, corn, pepper, wheat, sugarbeet, and rice.

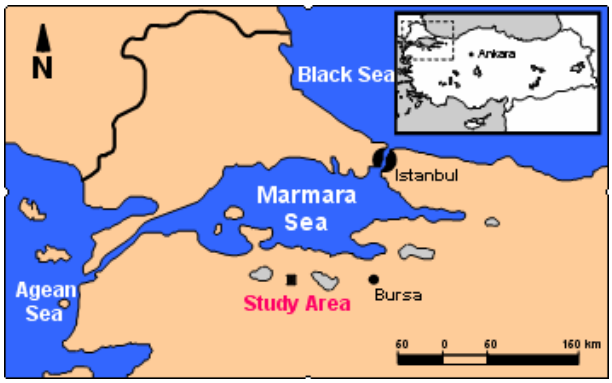


Figure 1. The Study Area

The field-based classification techniques require vector data to be integrated with the raster data. In this study, the vector field boundary data used was digitized for a previous thesis study conducted in the department of Geodetic and Geographic Information Technologies at Middle East Technical University (Arikan, 2003). Therefore, the vector field boundary data set was already available.

To perform the field-based classification operation, five different satellite images were used. These are SPOT4 XS (23 July 2004), SPOT5 XS (22 July 2004), IKONOS XS (15 July 2004), and QuickBird Bundle (13 August 2004). The acquisition dates of the images were kept as close as possible to each other. There was no effect for limiting the usefulness of the images. Each scene was collected at good weather conditions, cloud free and of good quality. The images were geocoded to Universal Transverse Mercator (UTM) coordinate system. The preprocessing level of the SPOT4, SPOT5, and QuickBird images was level 2A. On the other hand, the level of the IKONOS image was standard geometrically corrected. At these processing levels, the radiometric correction is made to compensate the distortions due to the differences in viewing conditions. The geometric correction is also applied on the images in a standard cartographic projection (UTM WGS 84) without using ground control points at the ground receiving stations. The technical characteristics of each image are given in table 1.

| | SPOT | IKONOS | QUICKBIRD |
|---|---|---|---|
| Processing L. | Level 2A | Std.Geo.Corrt. | Level 2A |
| Image Type | Multispectral | Multispectral | Bundle |
| Datum | WGS 84 | WGS 84 | WGS 84 |
| Map Projection | UTM | UTM | UTM |
| Zone Number | 35 | 35 | 35 |

Table 1. The technical characteristics of the images.

Of the images used, SPOT4 XS image has 20-m resolution and four bands that are green (G), red (R), near-infrared (NIR), and short wave infrared (SWIR). The area covered by the SPOT4 XS image is 556 x 461 pixels. The spatial resolution of the SPOT5 XS image is 10 m in the visible and NIR bands, while it is 20 m for the SWIR band. The size of the SPOT5 image used was 1120 x 929 pixels. The IKONOS XS image has 4 m spatial resolution. It contains four multispectral bands that are B, G, R, and NIR. The size of the IKONOS image was 2771 x 2324 pixels. The QuickBird Bundle standard product was also used in this study. The bundle product means that the panchromatic (PAN) and multispectral (XS) images are commerced together. The spatial resolutions of the QuickBird PAN and QuickBird XS images are 0.61 m and 2.44 m, respectively. The QuickBird images contain four XS bands (B, G, R, and NIR) and a PAN band. The sizes of the QuickBird images were 19026 x 15948 pixels for the PAN band, and 4666 x 3873 pixels for the XS bands. The spatial resolutions of the images used are illustrated in figure 2.

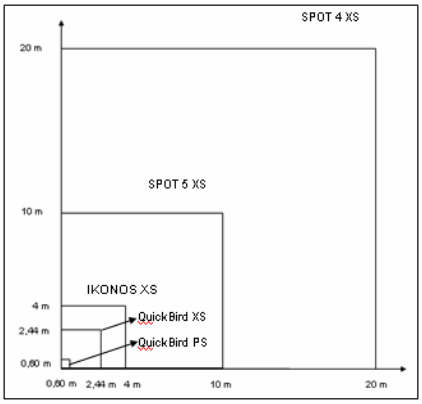


Figure 2. The spatial resolutions of the images.

## 3. PREPROCESSINGS

The vector data covering the study area was extracted from the existing file. Then, within field dynamic sub-boundaries were delineated through on screen digitizing, which was carried out using the colour composite of the NIR, R, and G bands of the QuickBird image. The SPOT5 XS image with the digitized vector field boundary data set overlaid is illustrated in figure 3.

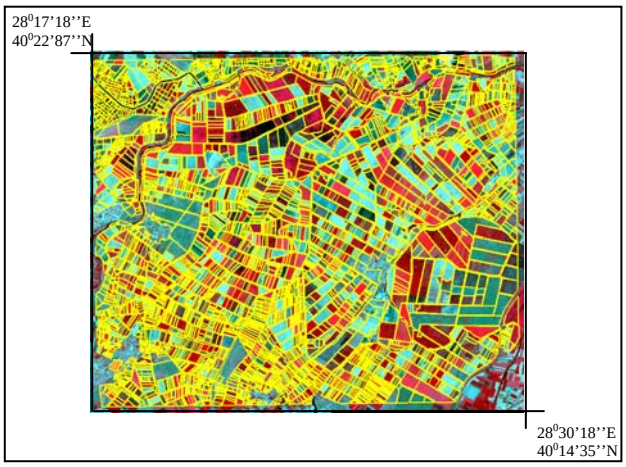


Figure 3. The SPOT5 XS image with the digitized agricultural field boundaries overlaid.

After completing the digitizing process, the number of fields increased from 3401 to 4134. In the study area, in addition to large fields, there were also a significant number of small fields. Next, the other pre-processing operations were carried out. These include image fusion, image-to-map geometric correction, and image-to-image registration. In order to test the accuracy of the high spatial resolution images, the QuickBird multispectral bands and the QuickBird PAN band were merged. The merged image retains the spatial resolution of the panchromatic band, yet provides the spectral properties of multispectral bands.

Although the images were acquired at different dates and sensor locations no additional radiometric or atmospheric corrections were carried out. One reason for this is that the sun elevation and the azimuth angles of the images were not significantly different. The azimuth angles of the SPOT4, SPOT5, IKONOS, and QuickBird images were $134{,}60^0$, $131{,}08^0$, $133{,}17^0$, and $141{,}60^0$, respectively. On the other hand, the sun elevation angles were $64{,}0^0$, $63{,}05^0$, $65{,}31^0$, and $59{,}60^0$, respectively. The other reason is that the purpose of this study was to separate the classes from each other through automated image classification. Therefore, radiometrically or atmospherically corrected image values do not dramatically affect the results (Janssen, 2005).

The geometric corrections of the images were carried out using a second-order polynomial and the nearest neighbour resampling techniques. The field boundary data set was used as the reference source. The GCPs were selected from distinct features, such as the intersections of the roads and sharp boundaries of the parcels. First, the QuickBird PS image was geometrically corrected based on the field boundary data. To do that 12 GCPs were selected from the same locations on both the vector and raster data sets. Second, the other images were registered based on the corrected QuickBird PS image. To perform these corrections, for each image, 20 GCPs were selected from the same locations. The results of the geometric corrections were quite satisfactory to perform the field-based classification procedure. For each image, the computed Root Mean Square (RMS) errors are illustrated in table 2 .

| Data | Number of GCPs | Polynomial | Resampling | RMSE (pixels) |
|---|---|---|---|---|
| SPOT4 XS | 20 | 2nd | NN | ± 0.40 |
| SPOT5 XS | 20 | 2nd | NN | ± 0.41 |
| IKONOS XS | 20 | 2nd | NN | ± 0.40 |
| QuickBird XS | 20 | 2nd | NN | ± 0.40 |
| QuickBird PS | 12 | 2nd | NN | ± 0.80 |

Table 2. The RMS errors for the geometric corrections of the images.

## 4. THE METHODOLOGY

### 4.1 Selecting the Training Areas

A great effort was spent when selecting the training areas since the training areas were collected from the most representative homogenous areas of the fields. The crop types selected to perform the classification include Corn (Cr), Residue (Rs), Sugarbeet (Sb), Rice (Rc), Tomato (Tm), and Pepper (Pp). We found that the spectral characteristics of tomato and pepper were quite similar. Therefore, these crops were aggregated and the resulting class was named as Tomato/Pepper (Tm/Pp). In addition to the spectral differences, the phenological characteristics of the crops were also taken into account when selecting the training areas. The phenological characteristics of the crops are given in figure 4 (Turker and Arikan, 2005).

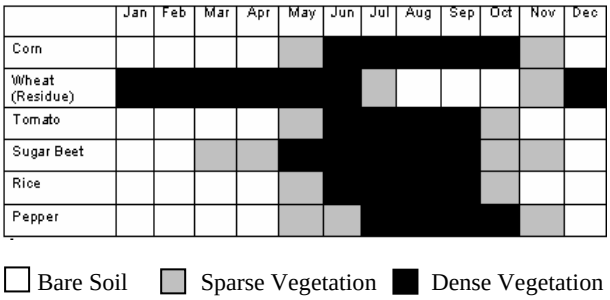


Figure 4. The phenological characteristics of the crops

The training areas were selected from the 4-m resolution IKONOS XS image. This is because the IKONOS XS image appears to be optimum for the visual selection procedure when compared with the other images. When selecting the training samples, the false colour composite of the bands 4 (NIR), 3 (R), and 2 (G) was used because the healthy vegetation absorbs most of the green and red incident energy and reflects almost half of the incident NIR energy. Therefore, the green vegetation shows up in shades of red.

### 4.2 Pre-Field Classification

In pre-field image classification, the statistical measures are calculated per-field and each field receives a unique spectral value. To apply this technique, the new bands that contain the mean, median, and mode values were generated using the common bands G, R, and NIR. By computing these statistical

values, a unique grey level was assigned to each agricultural field. Next, the derived new bands were used for performing the conventional maximum likelihood classification. The steps of the pre-field classification procedure are given in figure 5. A part of the output of the classification performed using the mean bands of the IKONOS XS image is illustrated in figure 6.

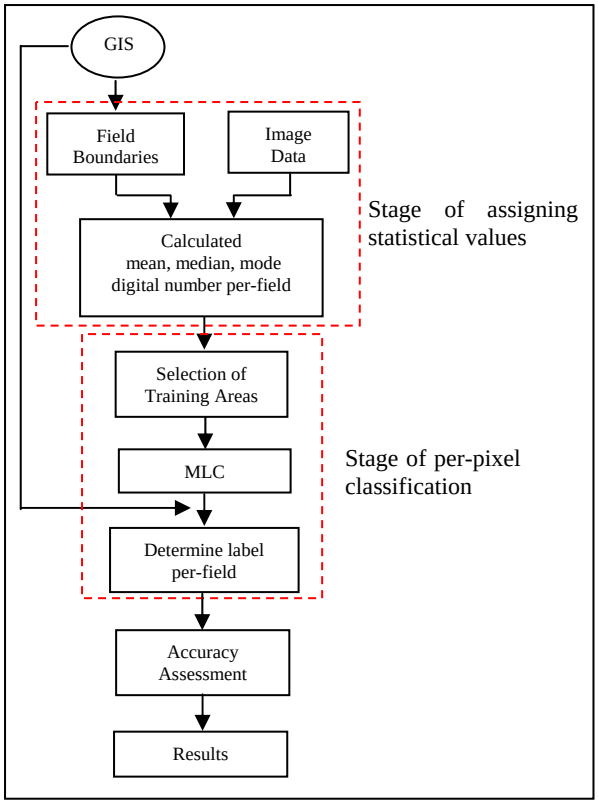


Figure 5. The pre-field classification procedure

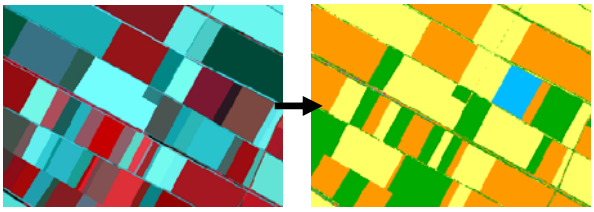

(a) (b)

Figure 6. For a part of the IKONOS XS image, (a) the color composite of the mean bands and (b) the output of the pre-field classification.

## 5. THE RESULTS AND DISCUSSION

For each image, the results were evaluated using an error matrix. For the mean values, the results are given in table 3. When the mean values were used, the highest overall accuracies were obtained for the QuickBird PS image. The overall accuracy and overall kappa were computed to be 82.1% and 74%, respectively. The highest individual accuracies of around 90% were computed for the class Rs. On the other hand, the lowest individual accuracies were obtained to be around 30% for the class Rc. The IKONOS XS image also provided high overall accuracies. For this image, the overall accuracy and overall kappa were computed to be 81.8% and 74.2%, respectively. While the highest individual accuracies (around 90%) were obtained for the class Rs, the other accuracies were marginal (around 75%). The QuickBird XS image provided the overall accuracy of 78.6% and overall kappa of 68.6%. Similar to the QuickBird PS image, the highest individual accuracies of approximately 90% were obtained for the class Rs. The lowest producer's and user's accuracies were computed to be 27.5% and 53.3%, respectively for the class Rc. For the SPOT5 XS image, the overall accuracy and overall kappa were computed to be 69.8% and 56.5%, respectively. While the highest user's accuracy of 97.1% was obtained for the class Rs, the lowest producer's accuracy of 45% was obtained for the class Rc. The SPOT4 XS image provided the lowest overall accuracy of 65.2% and overall kappa of 50.8%. When the individual classes were examined it was observed that the highest user's accuracy of 81% was obtained for the class Sb. On the other hand, the lowest producer's accuracy of 13.7% was computed for the class Rc, which provided the highest user's accuracy of 100%.

| | SPOT4 XS | | SPOT5 XS | | IKONOS XS | | QuickBird XS | | QuickBird PS | |
|---|---|---|---|---|---|---|---|---|---|---|
| | OA | OK | OA | OK | OA | OK | OA | OK | OA | OK |
| | 65,2 | 50,8 | 69,8 | 56,5 | 81,8 | 74,2 | 78,6 | 68,6 | 82,1 | 74 |
| | PA | UA | PA | UA | PA | UA | PA | UA | PA | UA |
| Rs | 56,3 | 96,3 | 72,8 | 97,1 | 84,9 | 97,9 | 93,2 | 89,1 | 94,8 | 90,1 |
| Sb | 81 | 36,1 | 81 | 56,6 | 97,2 | 69,2 | 43,2 | 64 | 54 | 68,9 |
| Rc | 13,7 | 100 | 62 | 60 | 65,5 | 82,6 | 27,5 | 53,3 | 34,4 | 27 |
| Cr | 78,2 | 69 | 45 | 75,1 | 77 | 76,2 | 62,4 | 91,5 | 71,9 | 89,5 |
| Tm /Pp | 66,4 | 54,1 | 84,4 | 57,3 | 82,2 | 75,5 | 94,1 | 69,7 | 91,7 | 79 |

PA: Producer's Accuracy (%), UA: User's Accuracy (%), OA: Overall Accuracy (%), OK: Overall Kappa (%)

Table 3. The accuracies of the pre-field classifications performed using the the mean bands.

For the median bands classification, the overall accuracy, overall kappa, and individual class accuracies are given in table 4. As can be seen in the table, the QuickBird PS image provided the highest accuracies. For this image, the overall accuracy and overall kappa were computed to be 85.2% and 78.8%, respectively. The lowest individual accuracies were found to be around 30% for the class Rc. The IKONOS XS image provided the overall accuracy of 80.2% and overall kappa of 71.7%. Similar to the QuickBird PS image the class Rc provided the lowest producer's and user's accuracies, while the accuracies of the other classes were around 80%. The QuickBird XS image provided the overall accuracy of 69.5% and a rather low overall kappa of 53.9%. When the individual class accuracies were examined, it was observed that all the Sb fields were classified as Tm and Pp. Therefore, non of the Sb fields were correctly classified providing a producer's accuracy of 0%. The second lowest producer's accuracy of 6% was computed for the class Rc, which provided a user's accuracy of 66.6%. For the SPOT5 XS image, the overall accuracy and overall kappa were computed to be 45.2% and 24.7%, respectively. The lowest producer's accuracy of 6% was obtained for the class Rs as of the 332 residue fields, 306 were omitted from this class. On the other hand, 95.2% of the residue fields, which were classified as Rs, actually represent the Rs category on the ground. For the median bands classification, the SPOT4 XS image provided the

lowest accuracies. For this image, the overall accuracy and overall kappa were found to be 42.9% and 21.7%, respectively. The lowest producer's accuracy of 9% was found to be for the class Rs. However, for this class, the user's accuracy (96,7%) was surprisingly the highest.

| | SPOT4 XS | | SPOT5 XS | | IKONOS XS | | QuickBird XS | | QuickBird PS | |
|---|---|---|---|---|---|---|---|---|---|---|
| | OA | OK | OA | OK | OA | OK | OA | OK | OA | OK |
| | 42,9 | 21,7 | 45,2 | 24,7 | 80,2 | 71,7 | 69,5 | 53,9 | 85,2 | 78,8 |
| | PA | UA | PA | UA | PA | UA | PA | UA | PA | UA |
| Rs | 9 | 96,7 | 6 | 95,2 | 83,4 | 97,1 | 68,9 | 97 | 95,8 | 88,5 |
| Sb | 21,6 | 72,7 | 35,1 | 86,6 | 94,5 | 85,3 | 0 | NaN | 86,4 | 61,5 |
| Rc | 34,4 | 24,3 | 31 | 56,2 | 48,2 | 60,8 | 6 | 66,6 | 31 | 28,1 |
| Cr | 79 | 30,5 | 88,5 | 31,1 | 75,1 | 73,5 | 93,9 | 58,9 | 76 | 92,6 |
| Tm /Pp | 50,9 | 70,7 | 52 | 83,9 | 81,9 | 73,2 | 58,8 | 77,1 | 92,5 | 85,8 |

Table 4. The accuracies of the pre-field classification using the median values.

The results of the mode bands classification are given in table 5. As can be seen in the table, the IKONOS XS image provided the best results. The overall accuracy and overall kappa were computed to be 81.9% and 74.2%, respectively. Of the producer's accuracies, the class Rc provided the lowest producer's accuracy of 58.6%, while the producer's accuracies of the other classes were computed to be around 80%. The highest user's accuracy of 96.7% was provided by the class Rs. The user's accuracies of the other classes were also remarkably high. For the SPOT5 XS image, the overall accuracy and overall kappa were computed to be 81.2% and 73.1%, respectively. While the user's accuracies of the classes Sb and Rc were marginal, the classes Cr, Tm/Pp, and Rs provided relatively high values. The class Rc provided the lowest producer's accuracy of 51.7% and a user's accuracy of 44.1%. The highest producer's and user's accuracies were obtained for the classes Tm/Pp and Rs. The QuickBird XS image provided an overall accuracy of 80.5% and an overall kappa of 71.7%. The lowest individual accuracies were obtained for the class Rc as it contains high omission and commission errors. Among the classes, Rs provided the highest producer's accuracy of 96.3% and a significantly high user's accuracy of 88.1%. For the QuickBird PS image, the overall accuracy and overall kappa were computed to be 69.7% and 53.9%, respectively. The highest producer's accuracy of 94.5% was computed for the class Cr. On the other hand, the class Rs exhibited a highest user's accuracy of 97.6%. Surprisingly the producers's accuracies of the classes Sb and Rc were found to be 0%. Unfortunately, no logical explanation could be made for this. The classification of the SPOT4 XS image provided the lowest accuracies. For this image, the overall accuracy and overall kappa were computed to be 48.2% and 28.8%, respectively. It was observed that the classes Rs, Sb, and Rc provided significantly low producer's accuracies while the accuracies of the classes Cr and Tm/Pp were marginal. For the class Rc, the user's accuracy was the lowest. On the other hand, the highest user's accuracy was computed to be 95.9% for the class Rs.

| | SPOT4 XS | | SPOT5 XS | | IKONOS XS | | QuickBird XS | | QuickBird PS | |
|---|---|---|---|---|---|---|---|---|---|---|
| | OA | OK | OA | OK | OA | OK | OA | OK | OA | OK |
| | 48,2 | 28,8 | 81,2 | 73,1 | 81,9 | 74,2 | 80,5 | 71,7 | 69,7 | 53,9 |
| | PA | UA | PA | UA | PA | UA | PA | UA | PA | UA |
| Rs | 14,1 | 95,9 | 77,7 | 98,4 | 89,4 | 96,7 | 96,3 | 88,1 | 63,7 | 97,6 |
| Sb | 18,9 | 70 | 59,4 | 66,6 | 86,4 | 84,2 | 37,8 | 58,3 | 0 | NaN |
| Rc | 24,1 | 12,9 | 51,7 | 44,1 | 58,6 | 80,9 | 34,4 | 29,4 | 0 | NaN |
| Cr | 81,6 | 34,4 | 77,8 | 86,8 | 77 | 72,6 | 68,7 | 90,4 | 94,5 | 58,9 |
| Tm /Pp | 60,3 | 75,9 | 91,6 | 72,4 | 80 | 76,6 | 91,4 | 76 | 61,8 | 78,3 |

Table 5. The accuracies of the pre-field classification using the mode values

The past studies have shown that a decrease in land-use/land cover accuracy is likely to occur when the spatial resolution of the data is improved (Townshed and Justice 1981; Toll 1984, 1985; Latty *et.al.* 1985; Martin *et. al.* 1998; Gong and Howarth 1990; Marceau et. al. 1994; Treitz and Howarth 2000). In this study, however, a decrease in pixel size resulted in an increase in the classification accuracy. For example, the QuickBird PS image provided the highest accuracies of about 85% for the classifications of the mean and the median bands. On the other hand, for the classification of the IKONOS XS image, the overall accuracies of about 80% were computed for each of the mean, median, and mode bands. For the SPOT4 XS image, the lowest accuracies were obtained for each of the derived bands. For the mean bands, the accuracies were calculated to be around 60%. When the median and the mode bands were classified, the overall accuracies were computed to be approximately 45%. The low classification accuracies of the SPOT4 XS image might have been caused by the heterogeneity of the fields. This means that the statistical values calculated for performing the pre-field classification may not represent the actual crop information within the fields due to the heterogeneity of the fields. The other reason would be the effect of the training pixels. It should be remembered that the training areas were selected from the IKONOS XS image and then transferred to other images so that the results could be compared more realiably. Therefore, the classifications were carried out using the samples collected from the same locations of the images. However, this was not quite possible due to the differences in the spatial resolutions of the images used. Depending on the spatial resolution of the images used the number of training pixels change. For example, the number of training pixels dramatically decreases for the SPOT4 XS and SPOT5 XS images. Therefore, for these images, the lower number of training pixels used in the classification might have resulted in low classification accuracies. The other reason would be the effect of small fields. It is known that, for the high spatial resolution images, higher number of pixels fall within the fields. Therefore, the small fields can be better classified using the high resolution images.

When the results of the individual class accuracies were examined it was observed that the class Rs provided the highest producer's and user's accuracies. This is due to the fact that the class Rs represents distinct spectral response pattern because when the images were acquired, the crop Rs had already been harvested. The other reason would be the size of Rs fields, which are quite large when compared with the fields of the other crop types. This means that higher number of pixels fall within the larger fields. Therefore, the number of the pixels to

be correctly classified may increase. In general, for each image, the class Rc exhibited the lowest accuracies, which may be due to the acquisition dates of the QuickBird images. The QuickBird images were acquired ten days after the acquisition dates of the other images. Therefore, the ten day time lapse might have had negative effects on both the quality of the training areas and the accuracy of the class Rc.

When the accuracies were examined with respect to the prices of the satellite images used a question of cost effectiveness raise, especially for image users to buy images under a fixed budget. For each statistic, a summary of the prices and the overall classification accuracies are given in table 6. As can be seen in the table, the cheapest of the four images used is SPOT4 XS, which has the cost of US$ 0,90km$^2$. The SPOT4 XS image appears to be cost effective for crop mapping. However, it provided an overall accuracy of 65.2%, 42.9% and 48.2% for the mean, median, and mode bands, respectively. Although the SPOT5 XS image was more than five times as expensive as the SPOT4 XS image, it provided about 30% better accuracy for the mode band and 5% better accuracy for the mean and median bands than the SPOT4 XS image. For all statistics, the IKONOS XS image provided an overall accuracy of about 80%. However, when the price of the IKONOS XS image is compared with the SPOT4 and SPOT5 images, a significant difference is evident. This is because the IKONOS XS image is almost more than five times as expensive as the SPOT5 XS image and more than thirty times as expensive as the SPOT4 XS image. The QuickBird images were the most expensive images used in this study. The cost of bundle product was US$ 32.00 km$^2$. The QuickBird PS imagery provided the highest classification accuracies of about 85% for both the mean and the median bands. On the other hand, a significant increase was not observed in the results of the mode bands classification, which provided the overall accuracy of 69.7%. Whereas the QuickBird PS imagery, the mode band classification of the QuickBird XS image exhibited relatively high accuracy of about 80%. The accuracies of the mean and median bands classifications were marginal, however.

| | Price/ km$^2$ | Mean Values | Median Values | Mode Values |
|---|---|---|---|---|
| SPOT4 | 0.90 | 65,2 % | 42.9 % | 48.2 % |
| SPOT5 | 5.50 | 69,8 % | 45.2 % | 81.2 % |
| IKONOS | 28.00 | 81,8 % | 80.2 % | 81.9 % |
| QuickBird XS | 31.00 | 78,6 % | 69.5 % | 80.5 % |
| QuickBird PS | 32.00 | 82,1 % | 85.2 % | 69.7 % |

Table 6. The costs and overall accuracies for each statistic.

## 6. SUMMARY AND CONCLUSIONS

In this study, field-based classifications were performed using the multi-resolution images of SPOT4 XS, SPOT5 XS, IKONOS XS, QuickBird XS, and QuickBird Pansharpaned (PS) covering an agricultural area located in Karacabey, Turkey. The classification of the median bands of the QuickBird PS image provided the highest overall accuracy of 85.2%. For the mean and mode bands classifications, the accuracies of 82.1% and 69.7%, respectively, were computed for the QuickBird PS image. The next highest overall accuracies of around 82% were computed for the IKONOS XS image using the mean and mode bands classifications and for the SPOT5 XS image using the mode band classification. For the IKONOS XS image, the overall classification accuracy was computed to be 80.2% using the median band. For the QuickBird XS image, the accuracy obtained for the mode band classification (80.5%) was similar. Unexpectedly, the classifications of the mean and median bands of the SPOT5 XS image resulted in rather low overall accuracies of 69.8% and 45.2%, respectively. The results of the SPOT4 XS image were also poor particularly for the median and mode bands classifications, which provided overall accuracies of 42.9% and 48.2%, respectively. For the classifications of the QuickBird XS image, the overall accuracies were computed to be 78.6%, 69.5%, and 80.5% for the mean, median, and mode values. Of the individual classes, the classification accuracies in excess of 90% were achieved for the class Rs. This is because the cover of a large number of fields is residue, which is easily separated from the other classes. On the other hand the lowest individual accuracies were obtained for the class Rc. The results achieved in this study showed that using the pre-field classification technique, remarkably high classification accuracies can be obtained for agricultural crop mapping. The results also showed that higher spatial resolution images provided higher classification accuracies.

**Acknowledgement**

The authors are grateful to State Planning Organization (DPT) of Turkey for supporting this project.

**References**

Arikan, M., 2003, A multitemporal masking classification method for field-based agricultural crop mapping. *Thesis in Geodetic and Geographic Information Technologies, Middle East Technical University, Ankara, Turkey*.

Chen D., Stow D.A., and Gong P., 2004, Examining the effect of spatial resolution and texture window size on classification accuracy: an urban environment case. *International Journal of Remote Sensing*, 25, 11, 2177-2192.

De Wit A. J. W., and Clevers J. G. P. W., 2004, Efficiency and accuracy of per-field classification for operational crop mapping. *International Journal of Remote Sensing*. 68, 11, 1155-1161.

Gong, P., and Howarth, P. J., 1990, The use of structural information for improving land-cover classification accuracies at the rural-urban fringe. *Photogrammetric Engineering and Remote Sensing*, 56, 67-73.

Janssen J., 2005, Introductory to Digital Image Processing: A Remote Sensing Perspective, Prantice Hall, United States of America, 198-199.

Latty, R. S., Nelson, R., Markham, B., Williams, D., Toll, D., and Irons, J., 1985, Performance comparison between information extraction techniques using variable spatial resolution data. *Photogrammetric Engineering and Remote Sensing*, 51, 1159-1170.

Lillesand T. M., Kiefer R. W. and Chipman J. W., 2004. Remote Sensing and Image Interpretation. Wiley, United States of America, 552-572.

Marceau, D. J., Howarth, P. J., and Gratton, D. J., 1994, Remote Sensing and the measurement of Geographical Entities in a forest environment 1: The scale and spatial aggregation problem. Remote Sensing of Environment, 49, 93-104.

Martin, L. R. G., Howarth, P. J., and Holder, G., 1998, Multispectral classification of land-use at the rural-urban fringe using SPOT data. *Canadian Journal of Remote Sensing*, 14, 72-79.

Smith G. M. and Fuller R.M., 2001. An integrated approach to land cover classification: an example in the Island of Jersey. *International Journal of Remote Sensing*, 22(16), 3123-3142.

Toll, D. L., 1984, An evaluation of simulated TM data and Landsat MSS data for determining suburban and regional land-use and land cover. *Photogrammetric Engineering and Remote Sensing*, 50, 1713-1724.

Townshend, J., and Justice, J., 1981, Information extraction from remotely sensed data, a user view. *International Journal of Remote Sensing*, 2, 313-329.

Treitz, P., and Howarth, P., 2000, High spatial resolution remote sensing data for forest ecosystem classification: An examination of spatial scale. *Remote Sensing of Environment*, 72, 268-289.

Turker M. and Arikan M., 2005. Sequential masking classification of multi-temporal Landsat7 ETM+ images for field-based crop mapping in Karacabey, Turkey. *International Journal of remote Sensing*, Vol. 26, No. 17, 3813-3830.